Discrete tunneling current fluctuations in metal–water–metal tunnel junctions

S. Boussaad and B. Q. Xu
Department of Electrical Engineering and Center for Solid State Electronics Research, Arizona State University, Tempe, Arizona 85287

L. A. Nagahara and I. Amlani
Physical Sciences Research Laboratories, Motorola Laboratories, Tempe, Arizona 85284

W. Schmickler
Abteilung Elektrochemie, University of Ulm, D-89069, Ulm, Germany

R. Tsui
Physical Sciences Research Laboratories, Motorola Laboratories, Tempe, Arizona 85284

N. J. Tao
Department of Electrical Engineering and Center for Solid State Electronics Research, Arizona State University, Tempe, Arizona 85287

(Received 23 January 2003; accepted 19 February 2003)

We have studied electron tunneling through water between two metal electrodes supported on a solid substrate and observed random fluctuations in the tunneling current between two discrete levels. The two-level fluctuations persist when changing the concentration and the valency of the ions, and *p*H of the water solutions. A given two-level fluctuation is, in general, not affected by the applied bias voltage, but it is usually disrupted by changing the width of the tunnel gap. We attribute the discrete conductance fluctuations to random trapping or escaping of a single electron in or from a localized state in the tunnel gap. © *2003 American Institute of Physics.*
[DOI: 10.1063/1.1566933]

INTRODUCTION

Electron tunneling through a solvent, such as water, is a fundamental process that plays critical roles in a variety of processes ranging from electrodeposition in electrochemistry to photosynthesis in biology. Despite intensive studies over the last several decades, a complete understanding is still lacking. Early theories that treat water as a continuous dielectric medium provide a reasonable description of many observed facts, but it cannot describe effects due to the discrete nature of the water structure and localized electronic states in water. Ultrafast laser spectroscopy studies have revealed the importance of localized states in water and other adsorbed layers on metal surfaces in the dynamics of electrons photoinjected from a metal surface.[1,2] We report here on a random discrete switching in the tunneling current through water between two fixed metal nanoelectrodes. The dependence of the switching on various experimental parameters, such as tunnel gap width, bias voltage between the electrodes, and salt concentration, suggests that the switching is due to tunneling via local states in the water layer. These local states are relatively close to the Fermi energy levels of the metal electrodes and thus play an important role in the electron tunneling through water.

To date, direct study of electron tunneling through a water layer between two metal electrodes has been performed using two approaches. In one approach, Porter and Zinn measured electron tunneling between two mercury spheres separated with a water film and observed evidence of layered water structure.[3] Because of the large size of the spheres, the number of water molecules in the tunnel junction is large. Another distinct feature of this approach is that the tunnel gap width is determined by the force between the spheres, due to the liquid state of mercury. The second approach is to use a scanning tunneling microscope (STM). The atomically sharp STM tip makes it possible to probe electron tunneling through a small number of water molecules between the tip and a conducting substrate.[4–6] The STM has provided valuable information about electron tunneling in water.[7–13] One of the unsolved puzzles is that the tunneling barrier height of the metal–water–metal junction measured by the STM is significantly lower than the vacuum counterpart. Despite the success, the tunnel gap in the STM is formed mechanically, which is prone to thermal drift, acoustic noise, and mechanical vibrations, thus making many measurements difficult. In the present work, we use electrochemically fabricated metal–water–metal tunnel junctions. Like the STM, each tunnel junction is formed between one or two protruding points from the electrodes, so the tunneling current is affected by a small number of water molecules. However, these tunnel junctions are supported on solid substrates and are thus immune to the instability and noise problems in the STM.

EXPERIMENTS

A critical requirement in our experiment is to fabricate stable electrodes that are separated with a tunnel gap ($<$ a

 © 2003 American Institute of Physics

Downloaded 22 May 2003 to 149.169.27.95. Redistribution subject to AIP license or copyright, see http://ojps.aip.org/jcpo/jcpcr.jsp

few nm).[14–16] We fabricated such nanoelectrodes using a self-terminated electrochemical method.[17] It starts with a pair of electrodes separated with a relatively large gap in an electrolyte. When applying a bias voltage between the two electrodes, metal atoms are etched away from the anode and deposited onto the cathode. As we found experimentally, the deposition on the cathode is localized to the sharpest point on the cathode, due to high electric field and metal ion concentration near the sharpest point. Consequently, the gap narrows and disappears eventually when the two electrodes connect. In order to form a desired tunnel gap between the electrodes, the etching and deposition processes must be terminated before final connection. We introduced a self-termination mechanism by connecting one electrode in series with an external resistor (R_{ext}) to form a voltage divider circuit. In the beginning, the gap is large and the tunneling across the gap is negligible, so the entire applied voltage falls between the two electrodes to drive the etching and deposition. As the gap narrows, the tunneling probability across the gap increases and the voltage between the electrodes drops as one expects for a voltage divider, which slows down the etching and deposition rates. Eventually, the etching and deposition terminate as the voltage becomes too small, which leaves us with a small gap between two facing electrodes. The final gap width is determined by R_{ext}. For a given R_{ext}, the terminal gap width varies from run to run, but it generally falls within a window of a few Å.

The starting electrodes mentioned above were fabricated in two methods. The first one is to manually glue a metal wire (99.999% Au, Cu, or Ag) with a diameter of 5–25 μm onto a glass slide with epoxy. The epoxy also serves as an electrical insulation layer required to reduce ionic leakage current. The wire is then cut with a razor blade to form a pair of facing electrodes separated with a gap of a few μm. The second method is to fabricate an array of Au electrode pairs on oxidized silicon substrate using optical lithography technology. Each electrode is 5 μm wide and 200 nm thick, which is connected to bonding pads for electrochemical etching and deposition as well as for electrical measurement. The electrodes in each pair point to each other with a separation of 1 μm. The electrodes are coated with a Si_3N_4 insulation layer except for a 5 μm$\times$5 μm window to expose a small portion of the facing electrodes to electrolyte. The leakage current is on the order 1 pA for a bias voltage of 0.1 V. The electrolyte was 0.1*M* HCl for Au electrodes, 0.1*M* HNO_3 for Ag, and 0.1*M* H_2SO_4 for Cu electrodes. After fabrication of the tunnel gaps with the self-termination method, we thoroughly rinsed the electrodes with 18 MΩ deionized water (Nanopure, Barnstead). The bandwidth of the measurement circuit is about 1 MHz, which allows us to probe the process as fast as 1 μs.

Rinsing with water does not necessarily remove all ions from the electrodes. In order to examine possible effects due to residual ions left on the electrodes, we performed the measurements using a STM setup (Pico-STM, Molecular Imaging Co.) in which the tunnel gap was formed mechanically between a tip and a substrate. The STM tip was formed by cutting a 0.25-mm-diameter Au (99.999%) wire, which was then coated with Apiezon wax to reduce leakage current well below 1 pA. The substrate was a Au film thermally evaporated on mica in vacuum (10^{-8} Torr), which was annealed and cleaned with a H_2 flame immediately before mounting it in a Teflon cell. The cell was boiled in piraha solution for 20 min. After rinsing it with a large amount of water, it was then boiled in deionized water for three times, each for 30 min. The $23\times\sqrt{3}$ reconstruction pattern of Au(111) was routinely observed. Drift in the STM during the experiment was 0.01–0.1 nm/s. We studied the time dependence of the tunneling current by temporarily suspending the STM feedback for 100 ms, and then reactivated the feedback to correct the tunnel gap due to drift. In comparison to the tunnel junction supported on a chip, the tunnel junction in the STM setup is less stable and the measured tunneling current is noisier. The STM has also a much lower frequency bandwidth ($\sim$10 kHz). These undesirable factors make a close study of the tunneling current rather difficult, but we have succeeded in detecting the discrete switching in the tunneling current, which allows us to rule out the possibility of residual ions as the origin of the switching. We note that the discrete switching does not affect STM imaging because it has a fast switching rate and small amplitude.

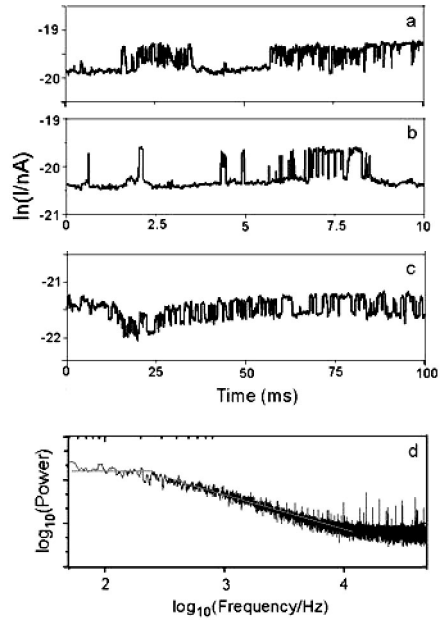

FIG. 1. (a) and (b) A typical time sequence of a two-level random switching in the tunneling conductance of a metal–water–metal junction on an oxidized Si chip. (c) Similar random switching observed in a tunnel junction formed between a Au STM tip and a Au substrate in water. (d) The power spectrum of a typical two-level switching. The bias voltage is 0.1 V.

RESULTS AND DISCUSSIONS

Figure 1(a) is a typical plot of the time dependence of the tunneling current in a Au–water–Au tunnel junction on a Si chip. It shows that the tunneling current fluctuates between two discrete levels, like telegraphic signals. A particular two-level fluctuation (TLF) such as the one shown in Fig. 1(a) usually lasts for a few to a few hundred ms. It will then disappear and be replaced with a another TLF, between two different levels [Fig. 1(b)]. We have observed the TLFs in the tunneling current using the STM setup although it is more

Downloaded 22 May 2003 to 149.169.27.95. Redistribution subject to AIP license or copyright, see http://ojps.aip.org/jcpo/jcpcr.jsp

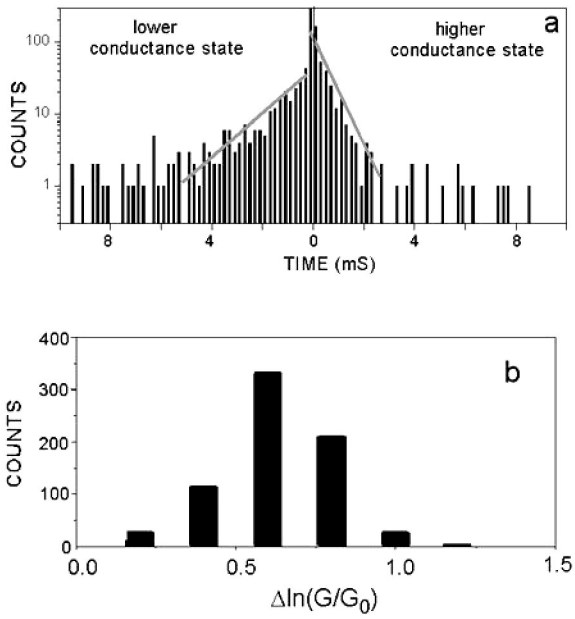

FIG. 2. (a) Histogram of time durations of the high and low conductance states. The counts are plotted in logarithmic scale, so the solid lines in the figure mark exponential dependence of the counts on the time duration. (b) Histogram of the switching amplitude. The switching amplitude in the plot is $\ln(G_{hi}/G_0)$-$\ln(G_{lo}/G_0)$, where G_{hi} and G_{lo} are the conductance values of two levels, and $G_0=2e^2/h$ is the conductance quantum. The histograms were constructed from over 200 time dependence curves of tunneling current.

difficult because of greater noise and instability [Fig. 1(c)]. Machlup proved that the power spectrum of random two-level events is a Lorentzian.[18] The power spectra of the TLFs in the tunneling current can be approximately described with a Lorentzian function, indicating that the sequence of the fluctuation events is random [Fig. 1(d)]. The time durations of the high and low tunneling states vary from a few μs to a few ms [Fig. 2(a)]. The lower limit was set by the limited bandwidth of our current amplifier, so we expect that faster switching events also exist but not detected. The distributions of time durations of the high and low tunneling states are plotted in Fig. 2(a). It shows that the occurrence of the fluctuations does not peak at a certain time duration; instead it decreases exponentially as the time duration increases. This indicates again that faster fluctuation events (shorter durations) are not recorded. The plot also shows that on average the high tunneling state has a longer time duration than the low conductance state.

The exponential decay observed in Fig. 2(a) indicates that the switching between the two conduction mechanisms follows a simple rate law for first-order kinetics. The distribution of the time duration is proportional to the distribution $P(t)$ of the reaction time, where $P(t)dt$ is the probability for a switch to occur in the time interval dt. For both directions this distribution takes the form

$$P(t)=A\ \exp(-kt\ ). \tag{1}$$

This can be related to the probability $Q(t)$ that a state persists till the time t:

$$Q(t)=1-\int_0^t P(t)dt=\frac{A}{k}\exp(-kt)+\left(1-\frac{A}{k}\right). \tag{2}$$

$Q(t)$ must vanish for long times; therefore $A=k$, and k can be identified with the rate constant. So the distribution of the reaction times is

$$P(t)=k\ \exp(-k\ t). \tag{3}$$

From the slopes in Fig. 2(a) we obtain a rate of $k_1=1.6\times10^{-3}\ \mathrm{s}^{-1}$ for the decay of the highly conducting state, and $k_2=0.7\times10^{-3}\ \mathrm{s}^{-1}$ for the reverse process. Since the rate constant enters also into the preexponential factor, we can obtain the ratio of the two rates also from the ratio of the intercepts; this gives $k_1/k_2=2.3$, which is in good agreement with the value obtained from the slopes. This confirms that the switching does indeed follow first-order kinetics. Further, from the ratio of the two rates we can estimate the difference between the free energies of the two states: the highly conducting state lies only about 0.02 eV higher than the other one.

For a given TLF, the amplitude or the difference between the high and low tunneling levels is fixed, but different TLFs can have very different amplitudes. The distribution of the amplitude is plotted in Fig. 2(b). The amplitude here is presented by $\Delta\ \ln(G/G_0)=\ln(G_{hi}/G_0)-\ln(G_{lo}/G_0)$, where G_{hi} and G_{lo} are the tunneling conductance of the high and low tunneling levels, which are normalized against $G_0=2e^2/h$, the conductance quantum. The plot shows a broad peak near $\Delta\ln(G/G_0)\sim0.5$.

A random fluctuation in the tunnel gap width could lead to a TLF in the tunneling current because of the dependence of the tunneling conductance (G) on the tunnel gap width (s),

$$G=G_0\exp(-\beta s), \tag{4}$$

where β is a parameter determined by the tunneling barrier between the electrodes. This was used to explain the stepwise change in the tunneling current between two electrodes during electrodeposition and etching.[19] However, under the condition of the present experiment, the probability of a fluctuating gap width caused by deposition and etching of metal atoms is low. Another possible change in the gap width is the diffusion of metal atoms on the electrode surfaces. This change in gap width should be comparable to the size of an atom or somewhat smaller if considering that the atoms do not stack on top of each other in three dimensions. However, using Eq. (1) with $\beta=10\ \mathrm{nm}^{-1}$ as determined experimentally by the STM,[10] the TLF amplitude shown in Fig. 2(b) can be as small as 0.01 nm, an order of magnitude smaller than the size of atom. Furthermore, if the surface atoms on the STM tip and the substrate were highly mobile, we would not be able to achieve atomic-resolution images.

Another mechanism that could change the tunnel gap width is the hydration force between the metal electrodes due to the ordering of water molecules in the tunnel gap. Porter et al. reported a stepwise increase in the tunneling current across a mercury–water–mercury tunnel junction as the two mercury electrodes approach each other.[3] The observation was attributed to a series of structural rearrangements of water molecules in the tunnel gap, causing an oscillatory hydra-

Downloaded 22 May 2003 to 149.169.27.95. Redistribution subject to AIP license or copyright, see http://ojps.aip.org/jcpo/jcpcr.jsp

tion force between the mercury electrodes and thus a discrete change in the electrode separation. As we have pointed out earlier, there are several important differences between the mercury tunnel junction and our system. First, the mercury tunnel junction has an area of $\sim 10^6$ nm^2, which means that the measured tunnel current is averaged over many molecules. In contrast, our tunnel gap is formed by a few atoms protruding out of the solid nanoelectrodes, which is sensitive to a small number of molecules in the gap. The small electrode area in our case means also a much weaker total oscillatory hydration force. Second, our electrodes are solid. Even if the oscillatory force did exist, it should not change the tunnel gap width as found for liquid mercury electrodes. Finally, the period of the oscillatory force is of the order of a water layer, which is an order of magnitude greater than we observed.

The above considerations, together with the fact that we have observed the same TLF with different electrodes (Au, Ag, and Cu), indicate that the TLF is originated from a process taking place in the tunnel gap. A number of processes in the tunnel gap may lead to such TLFs in the tunneling. An obvious one is the transient trapping of ions in the water layer between the metal electrodes. The presence of even a single metal ion in the tunnel gap can significantly change tunneling barrier due to large electrostatic potential and cause a large fluctuation in the tunneling current. Schmidlin showed that the trapping of a single ion in the tunnel gap of a metal–oxide–metal tunnel junction can change the tunneling current by one order of magnitude.[20] In order to examine the possibility of ion trapping as the origin of the TLF, we performed the measurement by introducing different ions into water (Na^+, K^+, Ca^{2+}, ClO^{4-}, SO_4^{2-}, NO_3^-, and Cl^- up to 0.5*M*). We found that the occurrence of the TLFs actually decreases somewhat in the presence of ions, which means that the observed telegraphic fluctuations in the tunneling current are not due to the trapping of ions in the tunnel gap. We note that, at high ionic concentrations, especially for divalent ions, we did observe intermittent noises with much larger amplitude in the tunneling current than the TLFs described here. These large amplitude noises are probably due to the transient appearance of ions in the tunnel gap, which is under investigation. We also performed the measurement in 0.1*M* $HClO_4$ and detected no obvious change in the occurrence of the TLFs, which rules out the *p*H (H^+ and OH^-) as the possible origin of the switching. We studied the TLFs using water with and without purging dissolved O_2 with N_2. In both cases, the occurrence of the TLFs is virtually the same, which eliminates the rule of dissolved O_2 in the TLFs. Finally, we measured the time dependent tunneling current in organic solvent (chloroform) and found that the telegraphic switching diminished. These observations suggest the TLFs are related to the water molecules in the tunnel junction, rather than foreign ions.

Water in the tunnel gap can affect the tunneling current via a change in the tunnel barrier. Since the potential energy profile of the tunneling barrier is determined by the local charge density that depends on the positions of the positively and negatively charged hydrogen and oxygen in water molecules, a fluctuation in the water configuration may change the tunneling current via a change in the tunnel barrier height. This fluctuation can be rather large because the tunnel barrier is determined only by a small number of water molecules. Recent molecular dynamics simulations indeed showed large variations in the tunneling current due to different water configurations.[21–23] For example, Schmickler found that different water configuration can change the tunneling probability by one order of magnitude.[21] Peskin *et al.* reported a large resonance enhancement in the tunneling current by the formation of a transient water cavity.[22] However, such structural fluctuation is extremely short lived according to the simulations, compared to the TLFs often observed on a ms time scale.[24]

In order to further examine this possibility, we studied the dependence of the TLF on the gap width. For this purpose, we used the STM setup, which allowed us to quickly and continuously change the gap width with a piezoelectric transducer (PZT). To avoid the STM tip from crashing into the substrate that can change the tip geometry, we ramped the set-point current while maintaining a small integral feedback gain. The feedback loop ignored the fast telegraphic switching but followed the ramping set-point value by driving the PZT up and down. In this way, the tunnel gap width was changed with minimal risk of crashing the STM tip into the substrate. Because of the intermittent nature of the telegraphic switching and also vibrations and noise in the STM measurement, only a small fraction ($<10\%$) of several thousand recorded time dependence of the tunneling current curves reveals clearly the telegraphic switching. Figure 3(a) is a typical such curve. It shows that a TLF at large distances between levels 1 and 2. Decreasing the gap width disrupts the TLF and results in new TLF between levels 2 and 3. Further decreasing the gap width switches the TLF to yet another one between levels 3 and 4. It is tempting to interpret the gap-width dependent TLFs to discrete rearrangements of the water configuration in the tunnel gap. However, we also observed (5%) that a TLF remains intact when changing the gap width over a range of several Å, comparable to the thickness of a water layer. Figure 3(c) shows such an example. Because the gap is wide enough to fit only 3–5 layers of water molecules, it is difficult to imagine that a water configuration remains unchanged when the gap width is changed over the large range, so random fluctuations in the water configuration are unlikely the origin of the TLFs. We note that although the TLF survives the change of the gap width both the fluctuation amplitude and rate do change with the gap width. For example, Fig. 3(c) shows clearly that the amplitude increases linearly as the gap width decreases. We will return to the explanation of this observation later.

Water in the tunnel gap can affect the measured tunneling current via providing local states in the tunnel gap. In fact, the presence of local defect states is known to give rise to two- or multiple-level telegraphic switching in metal–oxide–metal tunnel junctions.[25–27] According to the model, a fluctuation in the tunneling current is associated with trapping (escaping) of a single electron in (from) a local state in the tunnel gap. The exponential dependence of the counts on the time duration and the asymmetric distribution of the time durations of the high and low conductance states of the

Downloaded 22 May 2003 to 149.169.27.95. Redistribution subject to AIP license or copyright, see http://ojps.aip.org/jcpo/jcpcr.jsp

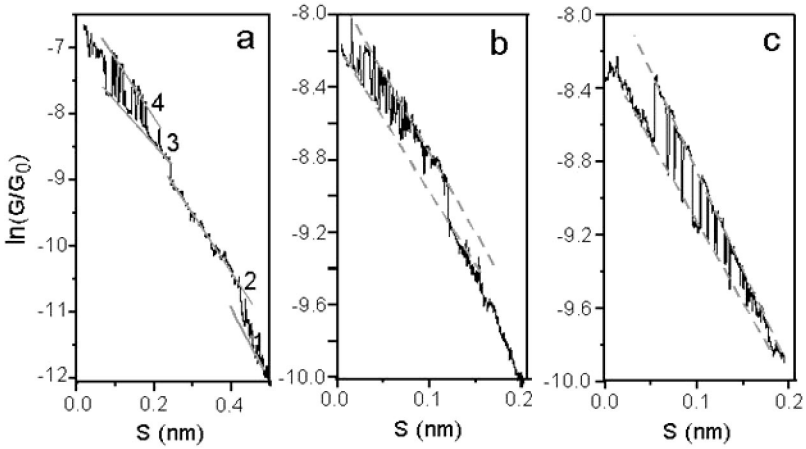

FIG. 3. (a) Typical dependence of a two-level switching on the gap width which is swept by applying a voltage to *z*-piezoelectric transducer in the STM setup, which shows that a two-level switch is usually disrupted by the change in the gap width. (b) A two-level switching can sometimes survive the change of the gap width over a fairly large range.

switching in our metal–water–metal tunnel junctions are remarkably similar to those observed in metal–oxide–metal tunnel junctions.[26,27] Based on these considerations, we propose that the TLFs in the tunneling current are due to the presence of local states in the tunnel gap. Figure 4 illustrates the process in the spirit of the Marcus theory.[28] Before electron trapping, an empty local state is positioned above the Fermi levels of the electrodes. Because of the strong coupling between the local state and the water molecules, a thermal fluctuation in the water configuration may move the local state closer to the Fermi levels. This will allow an electron from the metal electrodes to occupy the local state. Following the occupation, the surrounding water molecules relax and move the occupied local state below the Fermi levels, which results in the trapping of the electron. The presence of the trapped electron in the tunnel gap raises the tunneling barrier due to electrostatic repulsion between the trapped electron and the tunneling electrons, which switches the tunneling current to a lower level. When a thermal fluctuation moves the occupied local state close the Fermi levels, the trapped electron can escape to one of the metal electrodes and the tunneling current switches back to the original level. The trapped electron can also diffuse out of the tunnel gap, which explains the short lifetime of a particular two-level switching. A new local state can form in the tunnel gap in a later time and gives rise to another two-level switching.

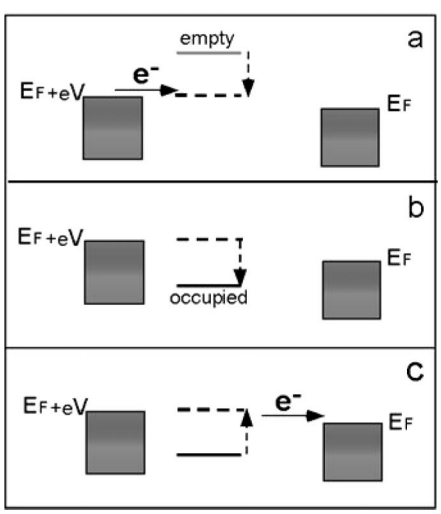

FIG. 4. Schematic illustration of a localized state model used to explain the observed two-level switching in the tunneling current. (a) An empty state localized in the tunnel gap is initially positioned above the Fermi levels of the electrodes. (b) When a thermal fluctuation brings the local state close to the Fermi levels, an electron can transfer from the electrodes and occupy the state. Relaxation of the surrounding water molecules will then move the occupied state below the Fermi levels. The trapping of an electron in the tunnel gap will lower the tunneling current due to electrostatic repulsion. (c) When a thermal fluctuation brings the occupied state back to the Fermi levels, the trapped electron can escape to the electrodes and empty the local state, which will cause the tunneling current to return to its initial value.

In addition to the basic observed facts described above, the model explains also all other observations. First, the average time durations of the high and low tunneling states are different. This asymmetry may be attributed to asymmetric positions of the empty and occupied states with respect to the Fermi energy levels. For example, if the empty state is closer to the Fermi levels than the occupied state, which means that the probability of trapping is higher than that of escaping, so the average time duration of the low tunneling state is longer than that of the high tunneling state. Second, it offers an explanation to the observed dependence of the TLF on the gap width. As we have described earlier, a particular TLF is usually disrupted by the change in the gap width, but it can sometimes survive the change over a large range. In the later case, the fluctuation amplitude is found to increase as the gap width decreases. According to the electron trapping model, the disruption of a TLF is because a trapped electron is either pushed to a new position or completely out of the tunnel gap. It is also possible that a trapped electron stays in the gap when the gap width is changed, which corresponds to the case when a TLF remains intact during the change of the gap width. The rapid increase in the switching amplitude in the later case can be explained by Eq. (1). If a trapped electron causes a change in the tunnel barrier height ($\Delta\beta$), then the corresponding switching amplitude is $\Delta G \approx e^{-s\Delta\beta}$, which should increase as the tunnel gap width decreases. Finally, the model explains the dependence of the TLF on the applied bias voltage (or *I*–*V* curves), which is described below.

Figure 5 shows the typical dependence of TLFs on the bias voltage. The average tunneling current is roughly a linear function of the bias voltage between -0.5 V and $+0.5$ V. When the bias voltage is swept over a wider range, the *I*–*V* curves become nonlinear, but leakage current due to polar-

Downloaded 22 May 2003 to 149.169.27.95. Redistribution subject to AIP license or copyright, see http://ojps.aip.org/jcpo/jcpcr.jsp

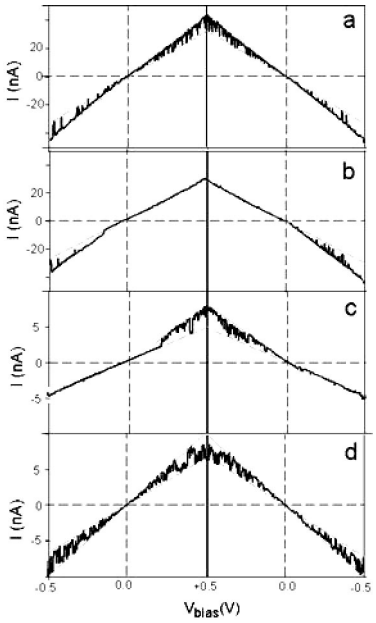

FIG. 5. Tunneling current vs applied bias voltage (I–V) which is swept from -0.5 V to $+0.5$ V and then back to -0.5 V. Three typical I–V curves (a)–(c) are presented here to show that the two-level switching can have different degrees of asymmetry, from high asymmetric in (a) to highly symmetric in (d). The asymmetry may be attributed to an asymmetric position of the local state in the tunnel gap.

ization and faraday process also increase. The amplitude of the TLF changes also linearly with the bias voltage, which means that the conductance values of the high and low tunneling states are not affected by the applied bias. Another important observation is that a TLF is usually not disrupted by the applied bias voltage, which is in contrast the dependence of the TLF on the tunnel gap width. The TLF is in general asymmetric with respect to the zero bias voltage. For example, Fig. 5(a) shows that the fluctuation rate increases when the bias voltage is swept from negative to positive values. This asymmetry is not accidental. When sweeping the bias back to negative, the fluctuation rate drops back again. More asymmetric I–V curves are shown in Figs. 5(b) and 5(c), where the fluctuations occur at either negative or positive bias only. Although most TLFs are asymmetric functions of the bias voltage, symmetric TLFs are occasionally observed [Fig. 5(d)]. The asymmetry of the TLF with respect to the bias is expected for an asymmetric position of the trapped electron in the tunnel gap.

We have recently observed a discrete conductance switching in a polyaniline nanojunction between two metal electrodes, which may be explained with a similar model.[29,30] However, there are two distinct differences between the polyaniline nanojunction and the present case. The first one is that the discrete switching in polyaniline exists even if the gap width is as large as 20 nm. Direct tunneling between two metal electrodes over such a large range is not possible, so electron transport must be through polyaniline in the gap. The second difference is that the switching probability in the polyaniline nanojunction corresponds to the oxidation and reduction of the polyaniline, which means that the local states are related to the redox states of polyaniline. The origin of the local states in the present case is less clear. The existence of local states in water has been proposed by several authors to explain the observed low tunnel barrier in the STM experiments.[9,10,22] In these models, the local states serve as intermediate states through which resonant tunneling of electron occurs. However, the microscopic origins of the local states proposed by different groups are quite different. We discuss below some possible origins of the local states.

One source of local states in the tunnel gap is surface states which include surface resonance state and image states. The energy level of a surface resonance state is usually close to the Fermi level for face-centered cubic transition metals, such as Au, Ag, and Cu used in this experiment.[31,32] Another important feature of the surface resonance state is that it is spatially located over several atomic layers of the electrode surface with a peak only slightly [$\sim$0.1 nm for Cu(111)] outside the topmost atomic layer. Because the surface resonance state is extremely close to the electrode surface, for a typical tunnel gap width (0.5–1 nm), the I–V curves must be always asymmetric. Since we have observed both asymmetric and symmetric I–V curves, the surface resonance state becomes unlikely. Image states arise from the attractive interaction between an electron outside of a metal surface and its induced charge on the metal surface, which is described as a mirror image of the electron. The attractive interaction leads to bound states localized several tenths of nm outside of the electrode surface.[31,32] At a metal–vacuum interface, the energy levels of these states are positioned several eV above the electrode Fermi levels. If one treats water as a continuous dielectric medium, they are even further above from the Fermi levels.[33] When we consider the existence of two electrodes, the attractive image potential of an electron in the tunnel gap is greater, which should shift the local states down towards the Fermi levels. This effect alone, however, does not seem to be enough to bring the states close to the Fermi levels. Another factor that can affect these surface states is that the tunnel gap is formed between two protruding points of the electrodes, rather by two perfect parallel surfaces. The discrete nature of water molecules may also affect the surface states. We point out also that the measured effective tunneling barrier height by STM is typically on the order of 1 eV, much lower than the vacuum value. If the surface states due to image potential are lowered proportionally, they would be close to the Fermi levels.

Another source of local states arises from water itself. The molecular orbitals of a single water molecule can be a source of local states, but their energies levels are much higher than the Fermi energy levels. Transient configuration of water molecules in the tunnel gap will also lead to local states. Recent molecular dynamics simulations by Nitzan's group have revealed that fluctuations of water molecules in the tunnel gap lead to transient cavities in the water structure which can dramatically enhance the tunneling probability via resonance effect.[22] These states still appear too high in energies, but, as they pointed out, other structural fluctuations that are not found in the finite time simulations may exist and lead to lower energy local states. Such configuration is ex-

Downloaded 22 May 2003 to 149.169.27.95. Redistribution subject to AIP license or copyright, see http://ojps.aip.org/jcpo/jcpcr.jsp

pected to be rare due to the cost of energy to form the cavity, but they may dominate the observed tunneling because their energy levels are close to the Fermi energy levels of the metal electrodes.

SUMMARY

We have observed a random fluctuation in the tunneling current of a metal–water–metal junction between two discrete levels. We have studied the fluctuations as a function of the tunnel gap width and applied bias voltage in pure water, organic solvent, and in the presence different ions of various concentrations. Our experimental results can be summarized as follows. (1) The two-level fluctuations (TLFs) are not greatly affected by the change of the concentration, valency of the ions, and *p*H of the solution. (2) A given TLF lasts for a few ms to a few hundred ms, and a new TLF between two different levels switches on at a later time. (3) The time durations of high and low tunneling states range from several a few μs to several ms. The lower limit is determined by the response time of the amplifier, and shorter durations are expect to exist but not detected. (4) The distributions of the time durations of the high and low tunneling states are asymmetric, although both fall quickly and monotonically with the time duration. (5) A given TLF is usually disrupted by the change of the tunnel gap width, but some of them can survive the change in the gap width. In the later case, the fluctuation amplitude change continuously with the gap width. (6) When we sweep the applied bias voltage, a given TLF usually survives, which is in sharp contrast to the change of the gap width. The amplitudes of the TLFs are linearly proportional to the bias voltage (between -0.5 and 0.5 V). The TLFs are usually asymmetric functions of the bias voltage. Our results can be explained by the existence a low-lying local state in the water layer between the metal electrodes. Each fluctuation event corresponds to the trapping of an electron in the local state, or to the escaping of the electron from the local state. However, the microscopic origin of the local state demands further experimental and theoretical efforts.

ACKNOWLEDGMENTS

We thank the DOE Grant No. (DE-FG03-01ER45943), EPA Grant No. (R82962301), and NSF Grant No. (CHE-9818073) and Stuart Lindsay for useful discussions.

[1] C. Gahl, U. Bovensiepen, C. Frischkorn, and M. Wolf, Phys. Rev. Lett. **89**, 107402 (2002).
[2] H.-H. Ge, C. M. Wong, R. L. Lingle, Jr., J. D. McNeil, K. J. Gaffney, and C. B. Harris, Science **279**, 202 (1998).
[3] J. D. Porter and A. S. Zinn, J. Phys. Chem. **97**, 1190 (1993).
[4] R. Gormer, Appl. Phys. A: Solids Surf. **39**, 1 (1986).
[5] M. Sumetskii and A. A. Kornyshev, Phys. Rev. B **48**, 17493 (1993).
[6] M. Sumetskij, A. A. Kornyshev, and U. Stimming, Surf. Sci. **307**, 23 (1994).
[7] M. Bingelli, D. Carnal, R. Nyffenegger, H. Siegenthaler, R. Christoph, and H. Rohrer, J. Vac. Sci. Technol. B **9**, 1985 (1991).
[8] J. W. Pan, T. Jing, and S. M. Lindsay, J. Phys. Chem. **98**, 4205 (1993).
[9] J. Halbritter, G. Reppphun, S. Vinzelberg, G. Staikov, and W. J. Lorentz, Electrochim. Acta **40**, 1385 (1995).
[10] A. Vaught, T. W. Jing, and S. M. Lindsay, Chem. Phys. **236**, 306 (1995).
[11] G. Nagy and G. Denuault, J. Electroanal. Chem. **437**, 37 (1997).
[12] G. Nagy, Electrochim. Acta **40**, 1417 (1995).
[13] Y. A. Hong, J. R. Hahn, and H. Kang, J. Chem. Phys. **108**, 4367 (1998).
[14] C. Z. Li and N. J. Tao, Appl. Phys. Lett. **72**, 894 (1998).
[15] C. Z. Li, A. Bogozi, W. Huang, and N. J. Tao, Nanotechnology **10**, 221 (1999).
[16] A. F. Morpurgo, C. M. Marcus, and D. B. Robinson, Appl. Phys. Lett. **74**, 2084 (1999).
[17] S. Boussaad and N. J. Tao, Appl. Phys. Lett. **80**, 2398 (2002).
[18] S. Machlup, J. Appl. Phys. **25**, 341 (1954).
[19] C. Z. Li, H. X. He, and N. J. Tao, Appl. Phys. Lett. **77**, 3995 (2000).
[20] F. W. Schmidlin, J. Appl. Phys. **37**, 2823 (1966).
[21] W. Schmickler, Surf. Sci. **335**, 416 (1995).
[22] U. Peskin, A. Edlund, I. Bar-On, M. Galperin, and A. Nitzan, J. Chem. Phys. **111**, 7558 (1999).
[23] M. Galperin, A. Nitzan, and I. Bengamin, J. Phys. Chem. A **106**, 10790 (2002).
[24] E. Spohr, Solid State Ionics (to be published).
[25] C. T. Rogers and R. A. Buhrman, Phys. Rev. Lett. **55**, 859 (1985).
[26] K. R. Farmer, C. T. Rogers, and R. A. Buhrman, Phys. Rev. Lett. **58**, 2255 (1987).
[27] X. Jiang, M. A. Dubson, and J. C. Garland, Phys. Rev. B **42**, 5427 (1990).
[28] R. A. Marcus, J. Chem. Phys. **24**, 966 (1956).
[29] H. X. He, J. S. Zhu, N. J. Tao, L. A. Nagahara, I. Amlani, and R. Tsui, J. Am. Chem. Soc. **123**, 7730 (2001).
[30] H. X. He, J. S. Zhu, N. J. Tao, L. A. Nagahara, I. Amlani, and R. Tsui (unpublished).
[31] N. Memmel, Surf. Sci. Rep. **32**, 91 (1998).
[32] A. D. Miller, I. Bezel, K. J. Gaffney, S. Carrett-Rose, S. H. Liu, P. Szymanski, and C. B. Harris, Science **297**, 1163 (2002).
[33] B. K. Clark, J. M. Standard, B. W. Gregory, and A. D. Hall, Surf. Sci. **498**, 285 (2002).

Downloaded 22 May 2003 to 149.169.27.95. Redistribution subject to AIP license or copyright, see http://ojps.aip.org/jcpo/jcpcr.jsp